JOURNAL OF MATERIALS SCIENCE 22 (1987) 1563–1572

Phase separation in blends of oligo(caprolactone glycol)-based polyurethane with poly(vinyl chloride)

V. V. SHILOV, V. N. BLIZNYUK, YU. S. LIPATOV
The Institute of Macromolecular Chemistry, Academy of Sciences, Ukrainian SSR, 252160 Kiev, USSR

The structure of oligo (caprolactone glycol)-based polyurethane-poly(vinyl chloride) (PVC) blends obtained from tetrahydrofuran solution was studied by X-ray diffraction and electron microscopy. The system is characterized by a complex phase diagram with two types of equilibria: (1) crystal–liquid equilibrium in the region of blend compositions up to 40 wt% PVC; (2) liquid–liquid equilibrium in the region of mean compositions. The crystallization kinetics of oligo(caprolactone) polyurethane blocks from an initially compatible amorphous blend was investigated. Small-angle X-ray scattering (SAXS) studies provide evidence that the amorphous component (PVC) is incorporated in the interlamellar crystalline regions of the compositions. The amorphous blends are characterized by the presence of modulated structures at two scale levels, this being explained as a result of the process in which the bulk samples were obtained from a three-component polymer–polymer–solvent system.

1. Introduction

The microphase structure of polymer–polymer blends is determined, as a rule, by thermodynamic conditions of phase separation and by the extent of this process completion [1]: Partially compatible blends with one crystallizable component are characterized by phase diagrams with a liquidus line. Phase separation in such systems occurs through nucleation and crystal growth with the formation of structures based on highly dispersed microcrystalline regions coexisting with the amorphous phase [2]. However, the diagrams of the state of systems with one crystallizable component are as a rule of a more complicated nature: the liquidus line is overlapped by the liquid–liquid phase equilibrium curve (binodal). It seems natural that the specific features of phase separation in similar systems depend to a considerable degree on the relative positions of the liquidus line and the binodal [3]. In particular, if the system is characterized by a binodal with the upper critical solution temperature (UCST) and the liquidus line is below the binodal on the temperature scale, then, on cooling, the crystallization of one of the components from the single-phase state should be expected to occur with a preliminary segregation of the liquid–liquid phase separation regions. Otherwise, in the case of a binodal with the low critical solution temperature (LCST) and the conditions being equal, the cooling is accompanied by a transition from a two-phase state into a single-phase state with a subsequent segregation of crystalline microdomains of the respective component. It could be expected that changes of a similar nature in the conditions of phase separation should be observed in a ternary polymer–polymer–solvent system on solvent removal.

Since the phase separation is frequently complicated by kinetic difficulties in mass transfer (mutual diffusion of polymers), especially with the approach to the glass transition region, it is difficult, even with the data on mutual position of phase equilibrium curves being accurate, to predict the microphase structure of the blend separated. If one considers that the accurate data on phase equilibria are not always available, then, to establish the microphase structure characteristics of binary polymer systems with amorphous and crystalline phase separation, the structure and morphology studies seem to be the only acceptable means.

Systems with amorphous and crystalline phase separation include also the partially compatible poly (ε-caprolactone) (PCL)–poly(vinyl chloride) (PVC) system [2, 4]. A binodal with low critical solution temperature (LCST) and a liquidus line are supposed to be present in this system [5]. Recently it has been shown that the PVC is partially compatible in a mixture with the polyurethane based on oligo (ε-caprolactone glycol) (PU(OCL)) [6]. This system is an example of polymer plasticization of poly(vinyl chloride), being at the same time an analogue of the PVC–PCL system with somewhat inferior compatibility of components. Some published data report on the structure and nature of the compatibility of this system components [6, 7]. Yet, the specific features of its phase separation are practically unknown. This work is aimed at studying the microphase structure of blends in the PVC–PU(OCL) system over a wide range of compositions due to the processes possible in the course of liquid–crystal and liquid–liquid phase transitions.

2. Sample preparation and experiments

PVC (molecular weight 140 000) and PU(OCL) based on oligo (ε-caprolactone) (molecular weight 2000) and diphenylmethane diisocyanate were chosen as initial components of the blends to be investigated. The PU(OCL) was synthesized according to technique described in [6]. The average viscosity molecular weight of the polymer obtained [8] was 48 000. The initial components of mixture compositions were reprecipitated and dried under vacuum. After that they were dissolved in the required proportion in tetrahydrofuran. Film samples were solution-cast over a Teflon substrate with subsequent solvent removal: first, for 8 h in the open at 323 K, then for three days under a pressure of ~ 1 torr at room temperature. The blend composition containing 75 wt % PVC was additionally annealed at 373 K (above T_g) for various time intervals.

Wide-angle X-ray diffraction (WAXD) studies of blends were carried out on an X-ray diffractometer DRON-2.0 in an automatic step scanning detector over the range of scattering angles 5 to 35° with a step of 0.2°. Small-angle scattering (SAXS) studies were conducted on diffractometer KRM-1 over the range of angles 0.2 to 3°, the step being 0.03°. In WAXD and SAXS investigations nickel-filtered copper anode radiation was employed. The experimental scattering curves were normalized to identical sample thickness with the X-ray radiation absorption taken into account [9]. Electron microscope studies were performed by the replica technique on an electron microscope JEM-100 C. Carbon replicas were taken from the sample surface etched in oxygen plasma [10]. To enhance the contrast, chromium shading and slight image defocusing were used [11]. The photographs were taken at an accelerated voltage of 80 kV and instrument magnification of 3 to 22 × 10^3. The size of the microdomains was determined using Fraunhoffer diffraction from electron microscopic patterns; the optical diffractometer IF-124 has been used which allows study of the spacial periods on patterns of size ~ 0.01 mm.

To determine the nature of the phase diagram, the cloud-point method was employed [12]. Samples were examined by the transmitted-light method using the MBS-9 microscope. The intensity of the transmitted light was recorded by a photoelectric multiplier. The rate of sample heating did not exceed 2 K min^{-1}.

3. Experimental results and discussion

3.1. Phase equilibria and glass transition

Fig. 1 shows the concentration dependence of the cloud point of the system investigated as compared to corresponding data for the PVC–PCL system [13]. As can be seen, the liquidus line (solubility curve) in the PVC–PU (OCL) system is lower, as compared to the PCL–PVC system, due to the presence of the diphenylmethane diizocyanate fragments in the polyurethane. Here, the last point in the solubility curve corresponds to 35 wt % PVC concentration. In the case of blends containing a greater amount of this component, the cloud points are not revealed, at least not in the visible region.

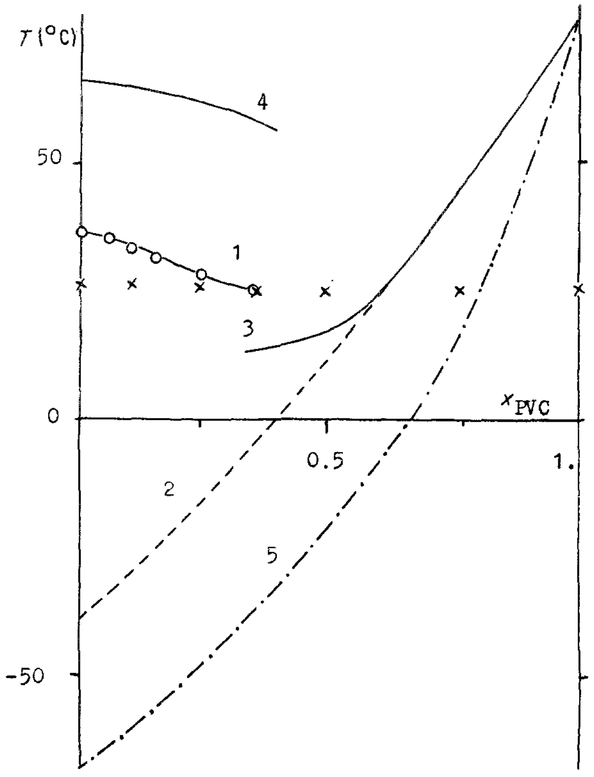

Figure 1 Phase diagrams: PU(OCL)–PVC system: 1, liquidus line; 2, additive glass transition temperature; 3, as 2, taking into account the component solubility limit (T_g was calculated as explained in the text). Compositions investigated are marked by crosses. The liquidus line (4) and the glass transition temperature line (5) for PCL–PVC blends are shown for comparison [13].

Thus, from Fig. 1 it follows that for both the PVC–PCL system and the PU(OCL)–PVC system the depression of the melting temperature in the crystallizing components occurs according to the parabolic law. This is characteristic of compatible polymer pairs with one crystallizable component [2, 12].

The thermodynamic interaction parameter of components χ_{12} was estimated by the Nishi and Wang technique [14] on the basis of the slope of the experimental dependence

$$\frac{1}{\phi_1}\left[\frac{1}{T_m} - \frac{1}{T_m^0}\right]$$

upon ϕ_1/T_m (ϕ_1 being the volume fraction of PVC; T_m and T_m^0 the melting temperatures of PU(OCL) in the mixture and in the pure state, respectively). In these calculations we used the values of the fusion enthalpy per mole monomer unit $\Delta H_m^0 = 0.55\,\text{kcal mol}^{-1}$ [8], the mole volumes of monomer units: PCL 86.7 $\text{cm}^3\,\text{mol}^{-1}$ and PVC 46.3 $\text{cm}^3\,\text{mol}^{-1}$. The latter values were calculated from density values: $\varrho_{PCL} = 1.20\,\text{g cm}^{-3}$ and $\varrho_{PVC} = 1.35\,\text{g cm}^{-3}$ [4]. This value proved to be close to zero ($\chi_{12} = 0.00 \pm 0.02$). For comparison it should be noted that the value χ_{12} found for the system PCL–PVC was equal to -0.31 [13]. Thus, the introduction of diphenylmethane diisocyanate links impairs the compatibility with PVC. From this point of view it seems probable that there may exist a region where two amorphous phases coexist at PVC concentrations above 35%. However, this surmise has not been supported by the above-mentioned results of cloud-point studies.

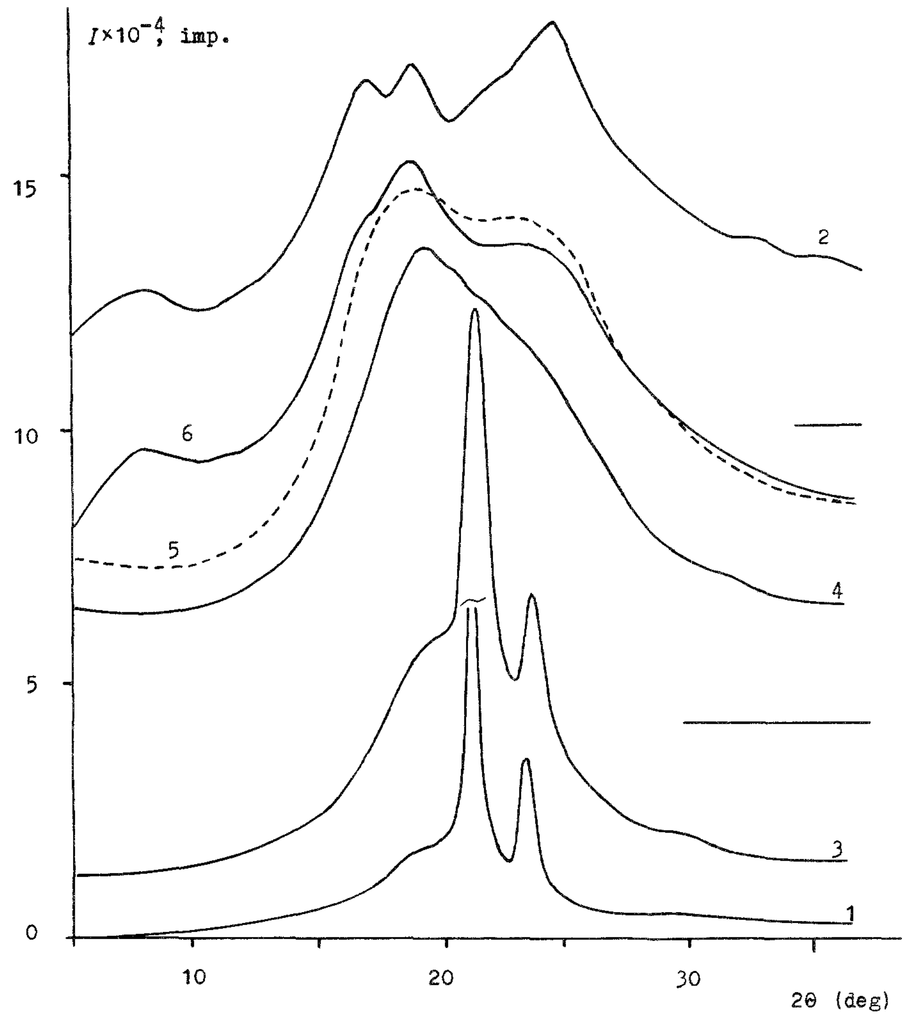

Figure 2 WAXD curves: 1, PU(OCL); 2, PVC; and blend samples: 3, 25 wt % PVC; 4, 50 wt % PVC; 5, 75 wt % PVC; initial (obtained from solution); 6, as 5, annealed for 30 min at 373 K. I = intensity of X-ray scattering, imp = impulse.

The next major characteristic of the blends investigated is the glass transition temperature. For the system investigated a corresponding concentration dependence was calculated by the Couchman method [15] taking into account the component solubility limit (which was taken to be 50% of PVC) and the literature data for the glass transition temperatures (PU(OCL), 234 K [7] and PVC, 353 K [12]). The curve obtained for T_g is given in Fig. 1. The concentration dependence of additive T_g values is shown in this Figure by a dashed line. For comparison, the glass transition curve PVC–PCL [13] is shown in this Figure by a dash-and-dot line. It should be noted that for the system under consideration the concentration interval corresponding to the glassy state at room temperature is much longer than that for the PVC–PCL system.

On the basis of the concentration dependences obtained T_m PU(OCL) and T_g of the blends in the phase diagram were selected as the most characteristic figurative points where we anticipated some interesting features of the microphase system state should be revealed at room temperature. These points (at PVC compositions of 10, 25, 35, 50 and 75 wt %) are marked in Fig. 1 by crosses. The first three points correspond to the equilibrium of the microcrystalline regions in the PU(OCL) and to the amorphous blend of the components. The fourth point is located in the amorphous state region very close to T_g. The last point (also in the amorphous region) corresponds to a temperature much lower than T_g, i.e. known beforehand to be the glassy state of the blend.

3.2. Fine structure of blends and liquid–crystal transition kinetics

Fig. 2 shows WAXD diagrams of the initial components of the system investigated and blends of various compositions. As can be seen, the pure PU(OCL) is characterized by a scattering curve typical of crystallizable polymers [7, 9]. The diffraction diagram reveals sharp crystalline reflexes and a superimposed halo representing the scattering from the amorphous phase. The locations of the crystalline reflexes are identical to the corresponding data for PCL and the initial OCL. Thus, the fine structure of PU(OCL) represents crystalline formations consisting of glycol chains and coexisting with the amorphous phase. The latter incorporates diphenylmethane diisocyanate fragments and some glycol chains not included in the crystallites.

In contrast to PU(OCL), the WAXD curves of the PVC signify the prevailing amorphous nature of the fine structure of this polymer. The intricate intensity curve profile may be considered as a result of scattering from a negligible amount of greatly distorted paracrystalline microregions incorporated into the amorphous matrix.

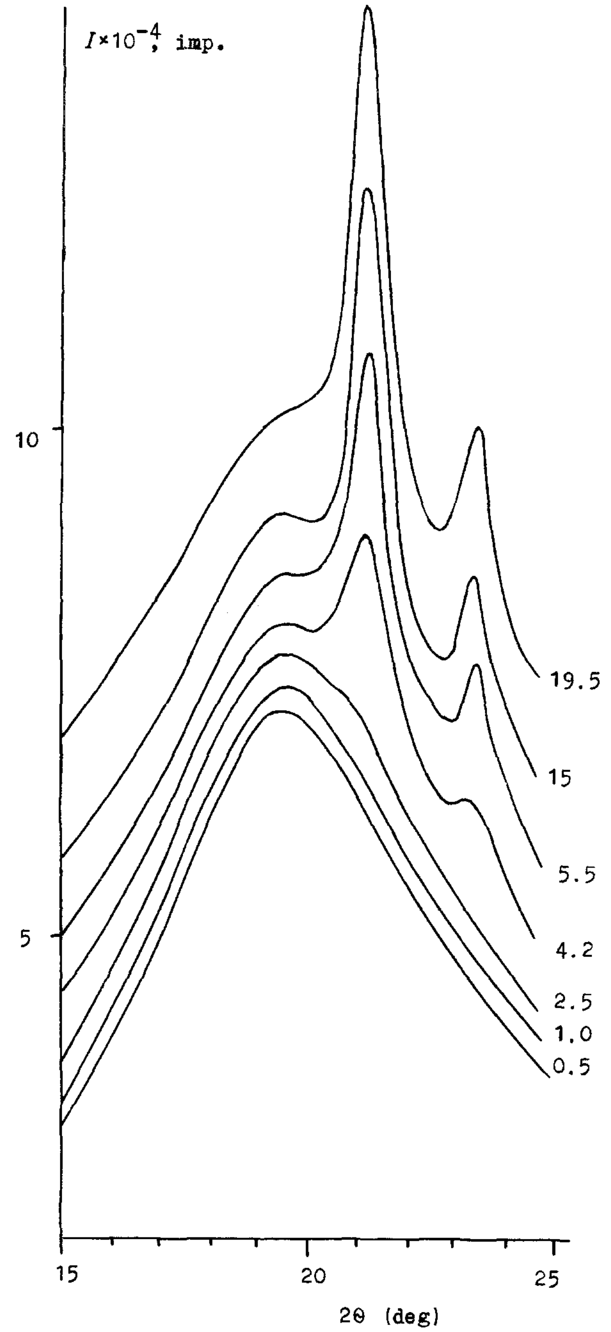

Figure 3 Appearance of crystalline PU(OCL) maxima during annealing of PU(OCL)/PVC = 75/25 sample quenched from melt to 273 K. The annealing time at T = 293 K in hours is indicated to the right of the diffraction diagrams. For better visualization, the curves are shifted along the ordinate axis.

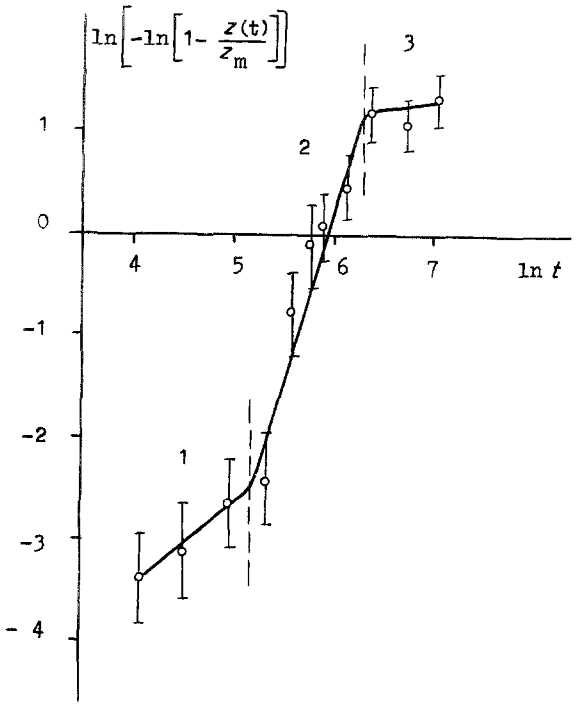

Figure 4 Phase separation kinetics of PU(OCL)/PVC = 75/25 blend: 1, 2, 3, phase separation stages (explained in text).

The WAXD curves for blends with 10, 25 and 35 wt % PVC (the latter is not shown in Fig. 2) are characterized by the presence of crystalline reflexes of PU(OCL). The intensity of the diffuse halo increases with the increase of PVC content. This is a natural reflection of the increase of the amorphous phase portion representing a blend of two components. On the whole the aforementioned blends are partly crystalline materials with segregated crystalline PU(OCL) domains.

The WAXD diagrams, as is well known, permit unequivocal establishment of the crystalline phase content of this or that polymer in a blend with amorphous high-molecular component [2, 9]. This offers a favourable possibility for the analysis of the crystallization kinetics of PU(OCL) from an amorphous blend with PVC. For this purpose we used a 25 wt % PVC blend made amorphous by quenching from 373 K into icy water. The crystallization kinetics was studied during sample annealing at room temperature the sample being kept in a wide-angle diffractometer chamber. The respective diffraction diagrams are shown in Fig. 3. As can be seen, with the annealing the crystalline reflexes of PU(OCL) appear against the background halo characteristic of the amorphous blend. These reflexes become apparent in 4 h following the quenching, then grow rapidly in the intensity. After 10 h following the quenching the growth of the number of crystallites practically ceases.

To study the overall crystallization kinetics, it is convenient to use the dependence

$$\ln\left[-\ln\left(1-\frac{Z(t)}{Z_m}\right)\right]$$

on ln t (Avrami coordinates) [16]. This dependence is shown graphically in Fig. 4 (t is the crystallization time in minutes; $Z(t)$, Z_m are the current and maximum values of the crystallinity index). The crystallinity index, Z, was determined as a ratio of the area under the crystalline peaks to the overall area of the wide-angle diffraction diagram.

In Fig. 4 three rectilinear sections can be discriminated, the slope of which determines the Avrami crystallization parameter, n. The first section ($n = 1$) is a characteristic stage of the phase separation by nucleation, i.e. the incubation period. At this stage the diffusion processes are predominant. At the second stage ($n = 3$) these processes are masked by strong three-dimensional crystallization dependence exp $[-kt^n]$. The third section is characterized by the perfecting of microcrystals following permeation of the crystallization front (secondary crystallization [16]).

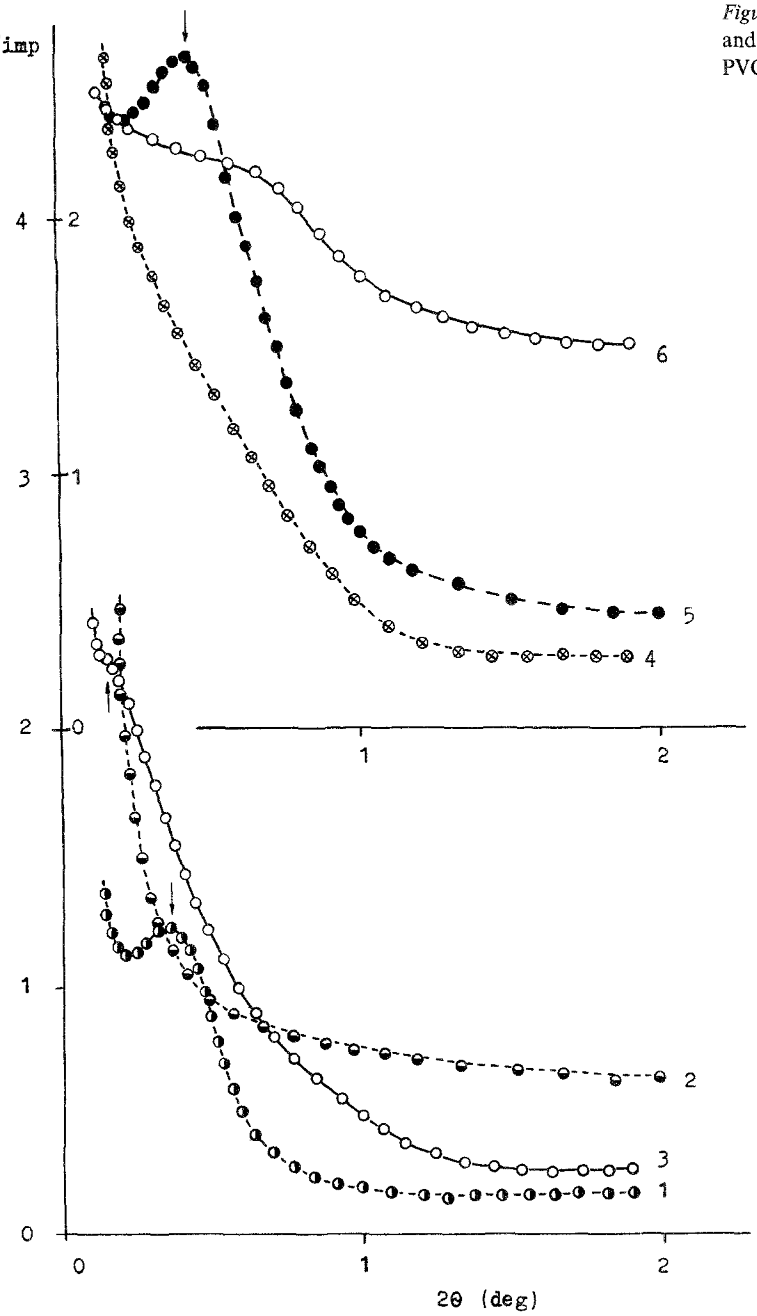

Figure 5 SAXS diagrams for: 1, PU(OCL); 2, PVC; and blend samples: 3, 25 wt % PVC; 4, 35 wt % PVC; 5, 50 wt % PVC; 6, 75 wt % PVC.

An important parameter characterizing the crystallization kinetics is the crystallization half-time, $t_{1/2}$, defined as the time required for the crystallinity degree to reach half the maximum value. From the above data it follows that in the PU(OCL)–PVC system the crystallization processes occur at an extremely slow rate, with the half-time of crystallization approximating 5 h (at $T = 300$ K). Apparently this is caused by the closeness of glass transition and crystallization temperatures resulting in retarded interdiffusion of PVC and PU(OCL) macromolecules.

Fig. 5 illustrates SAXS curves for the initial components of the system under consideration and blends of various compositions. It can be noted that in the case of pure PU(OCL) the diffraction curve displays a discrete maximum indicating ordered arrangement of crystalline microregions with amorphous spacings between them, i.e. with a characteristic long period *L*. Evidently, for this polymer, as for the majority of flexible-chain crystallizable high-polymers (among them PCL, which is of nearly the same nature), lamellar morphology is characteristic in the isotropic state [4, 9].

3.3. Short-range order and phase separation of amorphous blends

Beginning with 50 wt % PVC, the shape of the WAXD curves (Fig. 2) changes drastically: it is impossible to reveal even some traces of a crystalline structure in PU(OCL).

The WAXD profile of a 50 wt % PVC blend has a shoulder in its right-hand slope corresponding to the angular position of the most intensive PVC maximum. The latter permits an assumption that at this PVC concentration there are local inhomogeneities in component distribution within the sample. However, this is not a sufficient enough argument to draw conclusions about a segregation in the blend of microregions with PVC concentrations.

More information with respect to phase separation is offered by a WAXD curve of a blend containing 75 wt % PVC: the abovementioned shoulder in it is more distinct. Additional annealing at 373 K (above T_g) makes it possible to observe in the WAXD curve practically all three maxima characteristic of pure PVC. This seems to prove definitely that, upon removal of the solvent, segregated domains consisting predominantly of PVC appear in the blend of this composition. As a result of annealing, these domains, by their composition, approximate pure PVC. Thus, regardless of optical transparency of the amorphous blends considered, the WAXD studies show that, at least at 75 wt % PVC, the system is within the binodal. Since the rise in temperature promotes the segregation of amorphous domains enriched with PVC to a greater extent than in the initial state, it can be supposed that we deal with a system for which the concentration interval of liquid–liquid phase separation broadens with temperature elevation, i.e. a binodal with a low critical solution temperature (LCST) is characteristic of this system.

3.4. Microphase structure of blends

Let us refer to Fig. 5 once more. The SAXS diagram of pure PVC has, in contrast to PU(OCL), an absolutely diffuse profile. The latter is typical of amorphous homopolymers [9]. Unusual here is a very high level of small-angle scattering (greater even than in PU(OCL) characterized by heterogeneity due to alternating amorphous and crystalline domains). Such features of the PVC small-angle scattering pattern should be attributed to the survival in this polymer of more or less ordered microregions. This conclusion is in full agreement with the wide angle X-ray diffraction data. Since the amount of ordered domains in PVC is extremely small, the SAXS curve does not exhibit any discrete scattering giving evidence for their ordered arrangement. High electron density due to the presence of chlorine atoms results in local differences in electron density being quite large by the absolute value. The latter may elucidate the comparatively high level of X-ray scattering at small angles and negligible PVC heterogeneity.

The presence of a discrete SAXS maximum is characteristic of the majority of blend compositions investigated. This, according to the small-angle scattering theory [9] and independent of the presence or absence of crystalline microregions, may be put in correspondence with a definite value of long period, L, yielding a specific size for the heterogeneous structure of compositions and giving evidence for a regular alternation of microregions of varying electron density. However, considering that the phase structures of blends containing 10, 25 and 35 wt % PVC and those containing 50 and 75 wt % PVC, differ considerably, their small-angle scattering peculiarities should be attributed to various causes. In the first case, as in the case of pure PU(OCL), the microphase structure determining the nature of the SAXS diagrams is revealed as alternating amorphous and crystalline microregions. In the second case, the high level of the small-angle scattering should be attributed to the presence of amorphous microregions with various PVC concentrations. As follows from the diffraction curves, such microregions also alternate in a regular way. Similar modulated structures, but on a larger micrometer scale, were observed by Takashi Inoue *et al.* [17] for a series of polymer blends of small molecular weight and close values of solubility parameters. The authors explain the observed phenomenon from the point of view of a spinodal decomposition system with conditions for its occurrence arising in the process of solvent removal.

Fig. 6 shows the dependence of long period values on the composition. Also illustrated in this figure are the concentration dependences of other characteristic parameters of the microphase structure of blends examined: half-widths of small-angle maxima, $I_{1/2}$, and scattering intensity at the curve tail, I_∞. Quantity $I_{1/2}$ characterizes the degree of perfection of the supermolecular organization (perfection of macrolattice formed by heterogeneity microregions) and I_∞ is proportional to a so-called specific surface area of the heterogeneous structure, i.e. the degree of its dispersity [9].

From Fig. 6 follows that the experimental data depend on the PVC content in a non-monotonic way. With the increase of PVC concentration from 0 to 25 wt % the long period value changes with the portion of this component. Further increase of PVC content results in a discontinuity in the L-on-concentration dependence graph. In the discontinuity region, L decreases more than three-fold. Further on,

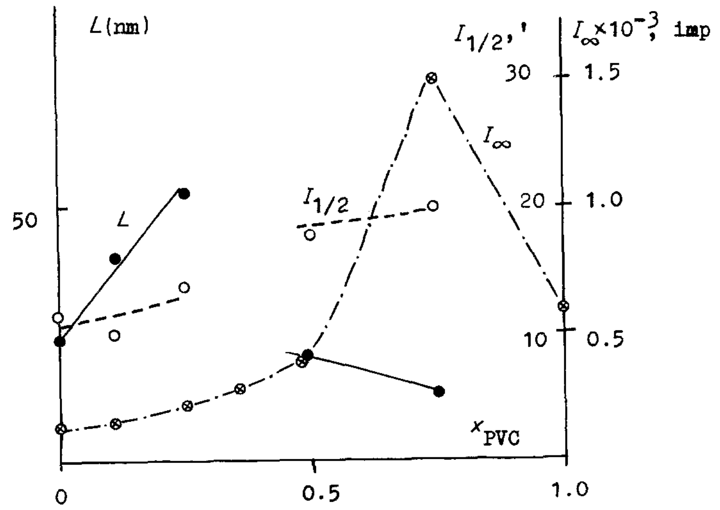

Figure 6 Dependence of SAXS parameters on the composition of PU(OCL)–PVC blends.

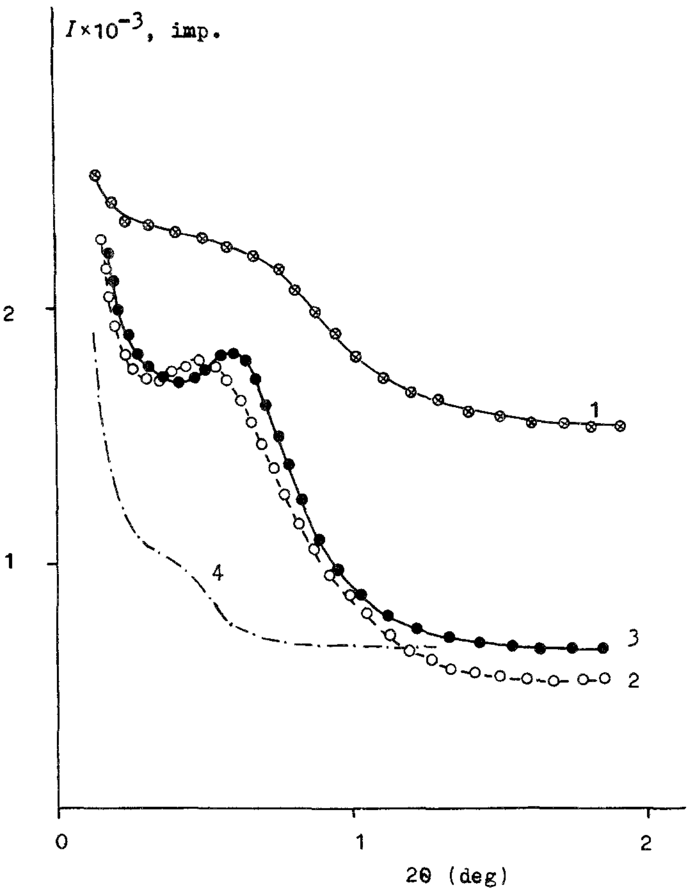

Figure 7 SAXS diagrams for PU(OCL)/PVC = 75/25 blend: 1, initial; 2, annealed for 15 min at 373 K; 3, as 2, for 45 min; 4, calculated additive curve.

up to 75 wt % PVC content, the long period value changes negligibly. Analogous discontinuity can be observed in the concentration dependence $I_{1/2}$: there are practically no changes in this value within the PVC concentration range from 0 to 25 wt %, after that it rises suddenly during the transition from 25 to 50 wt % PVC and remains almost unchangeable with further increase of this component content.

In contrast to L and $I_{1/2}$, the value of the specific surface area, with the increase of PVC content from 0 to 50 wt %, grows slightly. During the transition from 50 to 75 wt % PVC content the rate of its growth rises. In pure PVC, I_∞ is almost three-times lower than in a blend containing 75 wt % of this polymer.

The increase of the long period value with the increase of the portion of the component compatible in the amorphous phase with the crystallizable one is a well-known fact. Similar behaviour is also characteristic of the PVC–PCL system [4]. This fact may be explained as a result of the incorporation of PVC macromolecules into the amorphous interlamellar layers of PU(OCL). In this case, as follows from Fig. 5, the perfect packing of PU(OCL) crystalline domains remains practically constant.

The drastic drop in the value of L cannot be explained within the framework of concepts about PU(OCL) lamellae parting. Thus, this fact should be considered as additional evidence of essential differences in the supermolecular structure of the two abovementioned groups of PVC–PU(OCL) blends. Apparently, the small-angle scattering maximum in the case of blends containing 50 and 75 wt % PVC should be attributed to the formation of an ordered set of microregions typical for the processes of liquid–liquid phase separation. The width of the SAXS maximum indicates that the extent of perfection of the forming macrolattice is lower than that in a partially crystalline PU(OCL) and in blends containing up to 35 wt % PVC. The differences in the microphase structure of the two mixture groups find no reflexion in the concentration dependence, I_∞ up to 75 wt % PVC content. A sudden increase of the mixture dispersity on attaining this concentration should be viewed as a result of the formation of very small microregions during phase separation by one of the well-known mechanisms: nucleation and growth, or spinodal decomposition [1, 12]. To analyse this in terms of the specific features of the phase separation process, let us examine the variations of the SAXS curves of a 75 wt % PVC blend at various annealing times.

Fig. 7 shows the corresponding curves for the initial mixture containing 75 wt % PVC, for mixtures annealed for 15 and 45 min, as well as an additive scattering curve calculated from SAXS diagrams for pure components. From Fig. 7 it is evident that, as a result of annealing, the SAXS maximum becomes sharper and shifts towards the smaller scattering angles at a drastic drop of the scattering intensity at the tail of the diffraction curve. These effects bear evidence that the annealing leads to an increase of the periodicity scale and to microlattice perfection. A simultaneous considerable decrease of the number of small heterogeneity domains may be considered as an indication that the annealing results in a sharpening of the function of domain size distribution during microphase separation [9]. Comparison of experimental SAXS curves of the blend with a corresponding additive curve reveals that the scattering intensity of a blended composition is much higher than that for the initial components. Hence, the microphase structure arising in an amorphous blend as a result of liquid–liquid phase separation is more heterogeneous (is characterized by greater local electron density differences) than that of the initial, partially crystalline, PU(OCL) and initial PVC.

The SAXS data obtained for 75 wt % PVC blend at various annealing times bear evidence that this blend and, probably, the 50 wt % PVC blend at room temperature are within the binodal with the low critical solution temperature (LCST). This conclusion is also confirmed by the results of the wide-angle X-ray diffraction studies considered above.

3.5. Specific features of phase separation in blends due to solvent removal

Let us dwell now on those features of the investigated amorphous blends which are associated with the phase separation mechanisms, provide a certain level of process development in phase separation and ensure a subsequent fixing of the microphase structure at room temperature.

If, after the transition into the metastable or unstable phase diagram region, the phase separation processes would develop unimpeded, a system could be obtained which would be separated (like the ordinary liquid mixtures) in two macrophases – an upper phase (in this case one enriched by PU(OCL) and a lower one (enriched by PVC). Under such circumstances no dependence could be expected between the system structure and properties and the phase separation mechanism and, naturally, it would be impossible to obtain the variety of morphological forms of the decomposing partially compatible systems which are usual for the polymer–polymer blends.

The features observed in the SAXS diagrams are evidence that, in contrast to mobile liquid blends, the processes of phase separation in the system studied do not run through to their completion, but are inhibited at the intermediate stages, when the separating microdomains are still negligible in size (of the order of 10 nm). The inhibition of phase separation processes is, naturally, associated with the proximity to the glass transition region (Fig. 1). At room temperature, as follows from the wide- and small-angle scattering data, the system is within the region of the binodal with the low critical solution temperature, the binodal presumably passing through the range of compositions between 35 and 50 wt % PVC. Since the presence of solvent enhances the compatibility of two high-molecular components [1], a situation could be assumed when, at a definite content of tetrahydrofurane (THF), a 50% PVC blend is a single-phase system, i.e. the binodal of PU(OCL)–PVC–THF is located above the figurative point with the coordinates (50 wt % PVC, 298 K). The presence of solvent (according to Fig. 1) also leads to a reduction in the glass transition temperature for this blend. The system concentration under gradual solvent removal is accompanied by both a simultaneous worsening of component compatibility and by the approach of the glass transition region. The closeness of the glass transition temperature of a binary blend to room temperature indicates that the diffusive motion of polymer chains is retarded only slightly up to the complete solvent removal. The low value of the interaction parameter indicates that the single-phase state becomes metastable or unstable at very high concentrations of polymer–polymer–solvent system. Precisely under these conditions the processes of phase separation set in, forming periodically arranged microregions of various compositions, this being reflected by the presence of a characteristic maximum in the SAXS diagrams. Here, even negligible deviations from the average composition lead to a local PVC concentration sufficient for glass transition of microregions enriched by this component.

It is well known that the liquid–liquid phase separation may take place either by the nucleation and growth or by the spinodal decomposition. In the first case practically pure seeds of the new phase should segregate at the nucleation stage. Considering that in the blend under investigation even negligible enrichment by a component with a high glass transition temperature (PVC) results in a retarded interdiffusion, it should be admitted that the possibility of nucleation and growth is practically negligible, i.e. the phase separation cannot set in up to the moment when an absolute instability of the single-phase state is attained. The latter supports the fact that the phase separation in these blends occurs through spinodal decomposition.

As is known, the initial stages of spinodal decomposition are characterized by the growth (in terms of intensity) of periodically arranged composition fluctuations at their constant sizes. In this case the glass transition of PVC-enriched microregions leads to microphase structure stabilization at a certain stage of its evolution into a two-phase state, i.e. under conditions when the composition of microregions is still far from the equilibrium (according to existing concepts the composition of microregions is close to the equilibrium when the microregion sizes are by an order greater than the initial ones [18]).

It seems that in a blend containing 75 wt % PVC, on the removal of solvent phase separation commences, long before a complete system concentration. This follows from the fact that the figurative point of the phase diagram (75 wt % PVC, 298 K) corresponds to a greater incompatibility of components than point (50 wt % PVC, 298 K). The glass transition in a 75 wt % PVC blend should also begin at incomplete solvent removal. Therefore, the microphase structure of this blend is determined by the conditions of phase separation in the polymer–polymer–solvent system. In this case the conditions necessary for nucleation and growth are not satisfied so that the phase separation in 75 wt % PVC blend should also run the course of spinodal decomposition. This is directly confirmed by the modulated nature of the microphase structure of the system formed. Since the phase separation starts in the concentrated solution under continuous solvent removal, a wide distribution of microdomain sizes in phase distribution is observed in blends formed at room temperature. Facilitated interdiffusion of components with annealing results in more uniform sizes

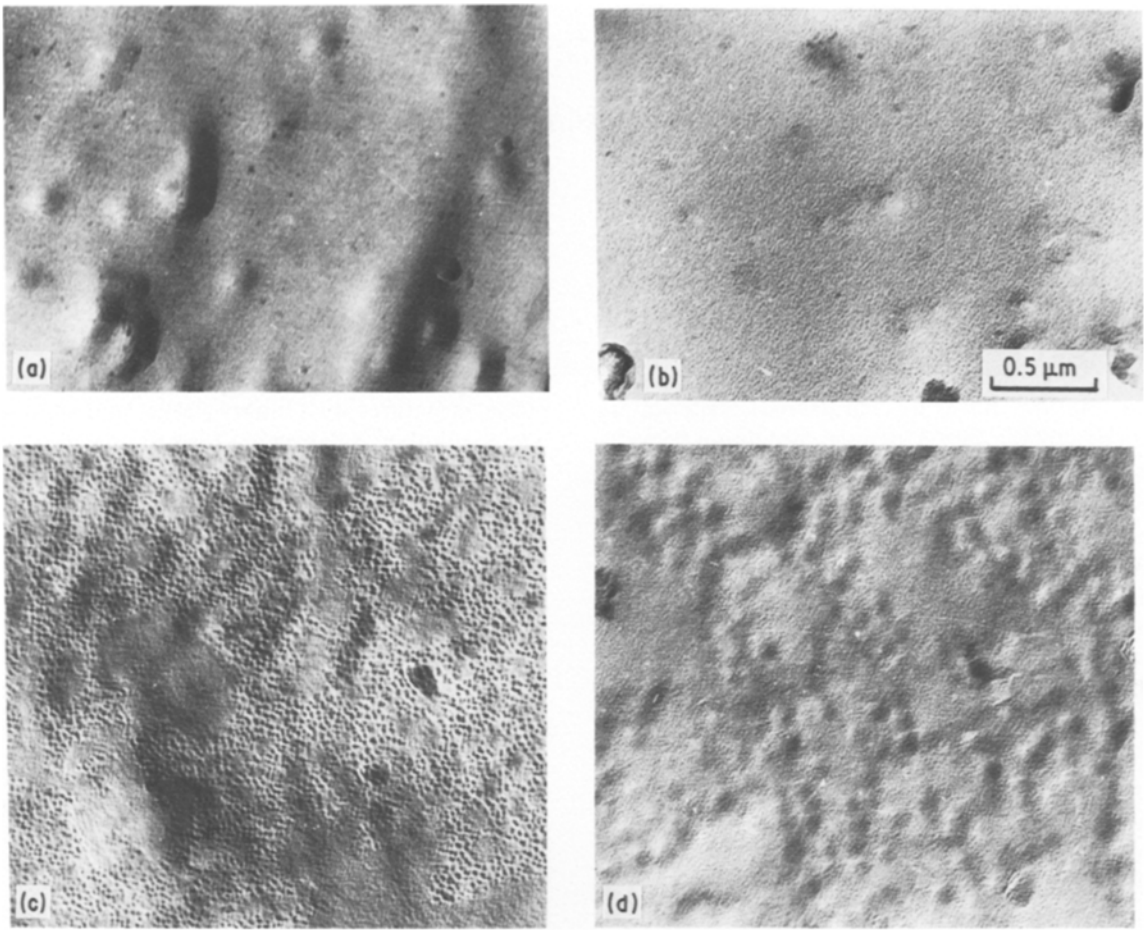

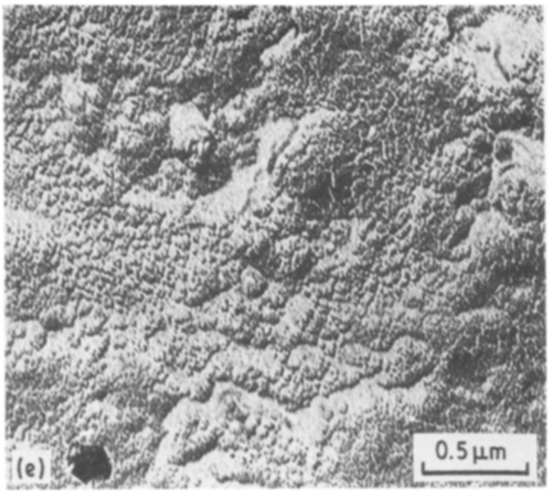

Figure 8 Electron micrographs of replicas from the surface of initial components: (a) PU(OCL); (B) PVC; and amorphous blends: (c) 50 wt % PVC, (d) 75 wt % PVC, initial, (e) as (d) after annealing for 30 min at 373 K.

of the microdomains and, correspondingly, in the stabilization of the system microphase structure at a stage characterized by a great phase separation depth and a more perfect modulated structure. Here, of importance is the fact that the compositions of the heterogeneity microregions are also far from the equilibrium, since the spinodal decomposition processes are retarded at too early a stage, before the disintegration of the modulated nature of the supermolecular structure.

3.6. The morphology of amorphous blends and phase separation

Fig. 8 shows the photomicrographs of replicas from the surface of initial polymers and blends containing 50 and 75% PVC, i.e. of amorphous systems. Electron-microscopic pictures of PU(OCL) and PVC show weak microheterogeneity of structure with a characteristic size of the order of 20 nm. Heterogeneity on the same scale is also exhibited in the photographs of the amorphous blends under consideration. It seems of interest to compare the sizes of heterogeneity regions found from optical diffractograms with corresponding values of long periods. The data are given in Table I. These data allow us to make a conclusion about qualitative agreement between size characteristics obtained using two different methods.

The specific morphology of amorphous blends displayed on a scale of the order of dozens of nanometres

TABLE I

Sample	Long period, L, determined by SAXS (nm)	Nodule sizes determined by electron microscopy (nm)
PVC	–	–
PU(OCL)	24.0 ± 0.2	–
PU/PVC = 50/50	20.4	18.5 ± 0.5
PU/PVC = 25/75, initial	13.0	13.5
PU/PVC = 25/75 annealed for 30 min at 373 K	15.5	15.0

depending on the conditions of phase separation, has been discussed in detail above. Principally, new information on the nature of heterogeneity on the scale of the order of 100 nm and more, unobtainable by X-ray diffraction analysis, is attainable by electron microscopy. In particular, in electron micrographs of blend compositions containing 50 and 75 wt % PVC, large microdomains are displayed which include up to several dozens of smaller ones. A photograph of a 50 wt % PVC blend clearly shows such supernodules, these being aggregates of small microdomains and regions free of them. The supernodules of the order 200 to 300 nm have a characteristic alternating periodicity. In the initial sample containing 75 wt % PVC spherical formations of a smaller size (~ 120 nm) are observed. On annealing their sizes diminish to 80 nm and the structure formed by them becomes extremely distinct. It should be noted that in all cases the morphological patterns formed by the system of the supernodules greatly resemble the interwoven structures observed in the spinodal decomposition of polymer–polymer blends [1, 12, 19]. Of significance is also the fact that their sizes are typical for systems based on macromolecular components [2, 12, 19, 20].

It is well known that in spinodal decomposition the spatial modulations of the composition are of a characteristic size, λ_m, dependent on the system's proximity to the spinodal according to the relation [2, 12]:

$$\lambda_m = 2\pi l \left[3 \left(\frac{T - T_s}{T_s} \right) \right]^{-1/2} \qquad (1)$$

where T_s is the temperature corresponding at given composition to the spinodal; and l is the distance of the intermolecular interaction.

From Equation 1 follows that, with the advance into the unstable region, λ_m diminishes. Then, assuming that in the system considered there exists a low critical solution temperature, the annealing should result in a decrease of λ_m. This has been confirmed by electron-microscopic studies. These data also indicate that with the transition from 50 wt % PVC blend to 75 wt % PVC blend, the withdrawal from the spinodal increases. Thus, at least at the qualitative level, the specific features of the "supernodular" morphology manifested in the electron micrographs may be considered as a result of the spinodal decomposition of the blends. Yet, the comparison of electron microscopic data giving evidence for a large-scale periodicity in blends containing 50 and 75 wt % PVC, and the results of small-angle X-ray scattering (the presence in these blends of small-scale composition modulations with a period lower by one order) does not permit one to obtain a classical pattern of spinodal decomposition. The nature of a double periodicity observed in amorphous blends is, most likely, associated with decomposition features of a system the composition (and, consequently, the phase equilibria) of which is constantly changing as a result of solvent removal.

4. Conclusions

It has been shown that the PU(OCL)–PVC system is characteristic of a complex type of phase equilibria involving the presence of the liquidus line and the binodal with low critical solution temperature. The glass transition region is close to the corresponding phase equilibria curves. As a result of this, the following specific features of phase separation were observed: in the forming of a binary blend by removing the solvent from a single-phase solution at a high content of the crystallizable component, a segregation of crystalline PU(OCL) phase is observed with a subsequent glass transition of the interlamellar blend layers; in preparation of samples enriched with PVC-stable microphase, structures with binary (large- and small-scale) composition modulation are formed as a result of the overlapping of the spinodal decomposition process under continuous blend concentration (and of the glass transition process).

Acknowledgement

The authors are grateful to V. A. Shrubovich for the synthesis of PU(OCL).

References

1. YU. S. LIPATOV, "Colloid Chemistry of Polymers" (Naukova Dumka, Kiev, 1984) p. 343.
2. D. R. PAUL and S. NEWMAN (eds), "Polymer Blends", Vol. 1 (Academic Press, New York, 1978) p. 549.
3. R. E. BERNSTEIN, C. A. CRAZ, D. R. PAUL and J. W. BARLOW, *Macromol.* **10** (1977) 681.
4. F. B. KHAMBATLA, T. RUSSELL and R. S. STEIN, *J. Polym. Sci. Polym. Phys. Ed.* **14** (1976) 1391.
5. O. OLABISI, *Macromol.* **8** (1975) 316.
6. P. K. BANDYOPADHYAY and M. T. SHAW, *J. Appl. Polym. Sci.* **27** (1982) 4323.
7. J. W. C. VAN BOGART, P. E. GIBSON and L. STUART, *J. Polym. Sci. Polym. Phys. Ed.* **21** (1983) 65.
8. V. CRSCENZI, G. MANZINI, G. CALZOLARI and C. BORRI, *Eur. Polym. J.* **8** (1972) 449.
9. YU. S. LIPATOV, V. V. SHILOV, YU. P. GOMZA and N. E. KRUGLYAK, "X-ray Methods of Analysis for Polymer Systems" (Naukova Dumka, Kiev, 1982).
10. E. V. LEBEDEV, YU. S. LIPATOV and L. I. BEZRUK, Analysis of Polymer Materials Morphology, in "New Methods in Polymer Investigations" (Naukova Dumka, Kiev, 1975) pp. 3–17.
11. D. L. HANDLIN Jr and E. L. THOMAS, *Macromol.* **16** (1983) 1514.
12. O. OLABISI, L. M. ROBESON and M. T. SHAW, "Polymer–Polymer Miscibility" (Academic Press, New York, London, 1979).
13. J. J. JISKA, J. W. BARLOW and P. R. PAUL, *Polymer* **22** (1981) 918.
14. T. NISHI and T. T. WANG, *Macromol.* **8** (1975) 909.
15. P. R. COUCHMAN, *Phys. Lett.* **A70** (1979) 155.
16. B. WUNDERLICH, "Macromolecular Physics", Vol. 2 (Academic Press, New York, 1976).
17. TAKASHI INOUE, TOSHIAKI OUGIZAWA, OSAMU YASUDA and KEIZO MIYASAKA, *Macromol.* **18** (1985) 57.
18. E. D. SIGGIA, *Phys. Rev.* **A20** (1979) 595.
19. L. P. McMASTER, "Advances in Chemistry Series 142 (American Chemical Society, Washington, 1975) pp. 43–65.
20. T. HASHIMOTO, J. KUMAKI and H. KAWAI, *Macromol.* **16** (1983) 641.

Received 17 September 1985
and accepted 11 February 1986